Anticancer effects of gemcitabine are enhanced by co-administered iRGD peptide in murine pancreatic cancer models that overexpressed neuropilin-1

Y Akashi[1], T Oda*[,1], Y Ohara[1], R Miyamoto[1], T Kurokawa[1], S Hashimoto[1], T Enomoto[1], K Yamada[1], M Satake[2] and N Ohkohchi[1]

[1]Department of Surgery, Clinical Sciences, Graduate School of Comprehensive Human Sciences, University of Tsukuba, 1-1-1 Tennoudai, Tsukuba, 305-8575 Ibaraki, Japan and [2]Department of Diagnostic Radiology, Research Center for Innovative Oncology, National Cancer Center Hospital East, Kashiwa, Chiba, Japan

Background: Impaired drug transport is an important factor that reduces the efficacy of anticancer agents against pancreatic cancer. Here, we report a novel combination chemotherapy using gemcitabine (GEM) and internalised-RGD (iRGD) peptide, which enhances tumour-specific drug penetration by binding neuropilin-1 (NRP1) receptor.

Methods: A total of five pancreatic cancer murine models (two cell line-based xenografts (CXs) and three tumour grafts (TGs)) were treated with either GEM ($100\,mg\,kg^{-1}$, q3d × 4) alone or GEM plus iRGD peptide ($8\,\mu mol\,kg^{-1}$). Evaluation of NRP1 expression in xenografts and 48 clinical cancer specimens was performed by immunohistochemistry (IHC).

Results: We identified a subset of pancreatic cancer models that showed NRP1 overexpression sensitive to iRGD co-administration. Treatment with GEM plus iRGD peptide resulted in a significant tumour reduction compared with GEM monotherapy in CXs, but not remarkable in TGs. Potential targets of iRGD were characterised as cases showing NRP1 overexpression (IHC-2+/3+), and these accounted for 45.8% of the clinical specimens.

Conclusions: Internalised RGD peptide enhances the effects of co-administered drugs in pancreatic cancer models, its efficacy is however only appreciable in those employing cell lines. Therefore, the clinical application needs to be given careful consideration.

Pancreatic cancer is one of the most intractable human malignancies, and the median survival of patients receiving the current standard therapeutic regimen with gemcitabine (GEM) is <6 months (Burris et al, 1997; Tempero et al, 2003). Insufficient therapeutic efficacy of anticancer drugs for solid tumours may be explained by the limited penetration of drugs into the cancer tissue (Ruoslahti et al, 2010). In fact, intravenously injected drugs are known to penetrate only a few cell diameters from blood vessels into the extravascular tumour tissue (Jain, 1999; Heldin et al, 2004). Therefore, a strategy for inducing drug hyperpermeability from tumour vessels might improve drug delivery to solid tumours.

Recently, a peptide known as iRGD (internalised-RGD) has developed (Sugahara et al, 2009, 2010). This peptide induces tumour-specific vascular hyperpermeability by binding to αv integrins that are specifically expressed on the endothelium of the tumour or angiogenic vessels. Co-administration of this peptide has been shown to markedly enhance the intratumoral accumulation of various agents with a wide range of molecular sizes in comparison with single administration, including doxo-rubicin (580 Da, 7-fold), dextran (1300–10 000 Da, 3- to 5-fold), Evans blue dye (66 000 Da, 2- to 4-fold), trastuzumab (148 000 Da, 40-fold), doxorubicin-liposome (Doxil, Janssen Pharmaceutica,

Beerse, Belgium) (120 nm, 14-fold), and nab-paclitaxel (abraxane; Abraxis BioScience, Los Angeles, CA, USA) (130 nm, 9- to 12-fold), in mouse breast or prostate cancer models (Sugahara *et al*, 2010).

Activation of circulating iRGD peptide requires interaction with neuropilin-1 (NRP1) (Sugahara *et al*, 2009). Intravenously administered iRGD peptide initially accumulates in tumour vessels by binding to endothelial αv integrin, and then its C-terminus is cleaved to expose an arginine or lysine residue (= C-end rule (CendR) motif), before drug penetration deeply into the parenchyma of solid tumours occurs through interaction with NRP1 (Sugahara *et al*, 2009; Teesalu *et al*, 2009). Neuropilin-1 is a multifunctional non-tyrosine kinase receptor that binds to class 3 semaphorins and the vascular endothelial growth factor (VEGF) family, playing essential roles in mediating axonal guidance and angiogenesis (Soker *et al*, 1996; Kolodkin *et al*, 1997). It is reportedly correlated with tumour progression and/or poor prognosis in various cancers, including pancreatic cancer (Parikh *et al*, 2003; Hansel *et al*, 2004; Li *et al*, 2004; Fukahi *et al*, 2004; Müller *et al*, 2007). However, as the clinical sample sizes evaluated were limited, that is, only 10 cases or less, the expression profile and prognostic significance of NRP1 in pancreatic cancer has remained unclear.

The characteristics of iRGD peptide in solid cancers seem to warrant further investigation, especially in those with a dismal prognosis such as pancreatic cancer. However, there have been no comprehensive *in vivo* studies using pancreatic cancer models, and the effects of iRGD peptide used in combination with GEM, a key drug employed worldwide for treatment of pancreatic cancer, have not been tested. In the present study, therefore, we examined the effectiveness of iRGD peptide for boosting drug accumulation in eight different mouse pancreatic cancer xenograft models. The anticancer booster effect of combination therapy with GEM plus iRGD peptide was evaluated with reference to *in vivo* experiments and analysis of NRP1 expression in clinical cases of pancreatic cancer.

MATERIALS AND METHODS

Drugs. The iRGD peptide (Sequence; CRGDKGPDC, disulphide bridge; C1–C9, Purity; >95%) we used for this study was delivered from a contract manufacturing company (American Peptide Company, Sunnyvale, CA, USA). A small quantity of the original iRGD peptide and control peptide (iRGE; CRGEKGPDC) were kindly provided by Drs Sugahara and Ruoslahti (UCSB, University of California, Santa Barbara), and the pharmaceutical power of our peptide was confirmed to be equivalent (data not shown). The other drugs purchased were Evans blue dye (MP Biomedicals, Santa Ana, CA, USA), dextran Alexa fluor 488 (D-22910, 10 000 Da MW; Molecular Probes, Eugene, OR, USA), and GEM (Gemzar; Eli Lilly, Indianapolis, IN, USA).

Cell lines and cell line-based models (= cell xenografts). The human pancreatic cancer cell lines AsPC-1 (CRL-1682), BxPC-3 (CRL-1687), and Capan-1 (HTB-79) were purchased from ATCC (Manassas, VA, USA). MIA PaCa-2 (JCRB0070) and SUIT-2 (JCRB1094) were purchased from JCRB Cell Bank (Osaka, Japan). AsPC-1, BxPC-3, and Capan-1 were cultured in RPMI-1640 medium (Sigma-Aldrich, MO, USA) with 10% fetal bovine serum. SUIT-2 and MIA PaCa-2 were cultured in Dulbecco's Modified Eagle Medium (DMEM; Sigma-Aldrich) with 5% and 10% fetal bovine serum. CXs were created by injecting these human pancreatic cancer cells (5×10^6 cells) into the dorsal subcutaneous space of C.B-17/Icr-scid/scid mice (female, 6 to 8 weeks old, CLEA Japan, Tokyo, Japan).

Transplant models using surgically removed tumour fragments (= tumor grafts). Pancreatic tumour grafts (TGs) were established by transplantation of fresh surgically resected tissue fragments of human pancreatic cancer. Samples were obtained under sterile

conditions, avoiding apparently necrotic tissue and areas of normal pancreatic parenchyma. The samples were cut into $2 \times 2 \times 2$ mm pieces, placed immediately in normal saline solution, and cooled on ice until implantation (usually within 30 min to 1 h). All human samples employed in the experiments were harvested after informed consent in documents, and the establishment and the experimental use of 'tumour grafts' were approved by laboratory animal resource centre at University of Tsukuba. More details about the methods and characteristics of TGs are described in our previous report (Akashi *et al*, 2013).

***In vivo* systemic permeability assay.** Tumour-bearing mice were injected intravenously with 100 μl of PBS containing either 1% Evans blue dye or 0.3 mg of dextran. Internalised-RGD peptide (100 μl, 12 μmol kg^{-1}) or PBS was also injected *via* the tail vein 10 min beforehand. After 30 min of circulation, the mice were perfused with PBS containing 1% BSA, and their organs were collected. For Evans blue quantification, the dye was extracted from whole tumour tissue collected from each mice in *N,N*-dimethyl formamide (Sigma-Aldrich) for 24 h at 37 °C and quantified by measuring the absorbance at 600 nm with a spectrophotometer and the measured results were normalised by the tumour weight (Sugahara *et al*, 2010). Harvest tissues after dextran administration group were immediately fixed with 4% paraformaldehyde for 24 h, frozen in optimum cutting temperature (OCT) solution, and stored at − 80 °C.

Immunofluorescence. Tissue specimens frozen in OCT solution were sectioned (5 μm thick), mounted on slides, and air dried for 30 min. The primary antibody was goat anti-mouse CD31 (AF3628; R&D Systems, Minneapolis, MN, USA), and the secondary antibody was anti-goat Alexa Fluor 546 (Life Technologies, Grand Island, NY, USA). The sections showing immunofluorescence were scanned with a microscope (BZ-9000; Keyence Japan, Osaka, Japan).

Quantification of dextran distribution. Dextran distribution was evaluated by arbitrary selected four hotspots per tumour. These hotspots were selected from the central area of the tumour including cancer cell nests, and avoiding the peritumoral stromal areas. The fluorescent area above a certain threshold in each 200 magnification field was calculated using the Image J software (v1.44p, Rasvand, National Institutes of Health, USA), and the measurement results were averaged.

Tumour treatment study. Mice bearing tumours (two CXs (BxPC-3 and MIA PaCa-2) and three TGs (PC-03, 09, and 10)) received an intra-peritoneal injection of GEM (100 mg kg^{-1}) or saline (100 μl) twice a week for 2 weeks. The treatment was combined with intravenous injection of iRGD peptide at 8 μmol kg^{-1} or PBS 10 min before GEM injection. The mice were weighed and tumour volume was measured twice per week. All xenografts were harvested 28 days after the start of treatment. Tumour volume was calculated using the formula: volume $(\text{mm}^3) = (d^2 \times D)/2$, where d is the smallest and D is the largest tumour diameter.

Clinical specimens of pancreatic cancer. Forty-eight consecutive patients, who underwent surgery for pancreatic cancer at Tsukuba University Hospital between September 2003 and April 2009, were included in the study. Histologically proven cases of pancreatic ductal adenocarcinoma were included, and cancers derived from intraductal papillary mucinous neoplasms were excluded. None of the patients had received neo-adjuvant chemotherapy or irradiation before surgery. Specimens of pancreatic cancer tissue obtained with the patient's consent were fixed in 10% formalin solution and embedded in paraffin. The pathological diagnoses and classifications were made on the basis of the UICC TNM classification of malignant tumours, 7th edition (Sobin *et al*, 2009).

Immunohistochemistry. Paraffin-embedded sections were deparaffinised in xylene and dehydrated through a graded ethanol series. The sections were heated in Tris-EDTA buffer (pH 9.0) for 10 min at 121 °C in an autoclave for antigen retrieval, and endogenous peroxidase was quenched in 0.03% hydrogen peroxidase for 15 min. The specimens were then incubated with the primary antibody: anti-NRP1 (sc-5307, 1:50; Santa Cruz Biotechnology, Santa Cruz, CA, USA) overnight at 4 °C, or anti-CD31 (LS-B1932; LifeSpan BioSciences, Seattle, WA, USA) for 1 h at room temperature. The remaining steps were carried out with the Envision+ System-HRP (DAKO, Glostrup, Denmark), followed by counterstaining with haematoxylin. Specificity of this antibody was verified by immunostaining of human kidney tissue samples. To assess tissue NRP1 expression, the sections were scored semi-quantitatively (on a scale of Immunohistochemistry (IHC)-0–3: negative = 0, weak = 1, moderate = 2, and strong = 3) according to the intensity of chromogen deposition in 10% or more of the neoplastic cells.

Microvessel density. Microvessel density (MVD) was measured by counting the number of CD31-positive blood vessels at selected
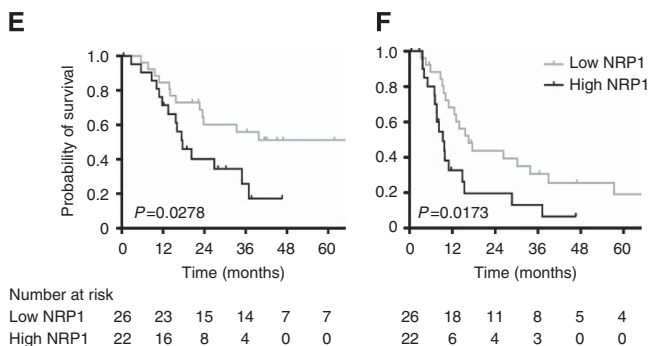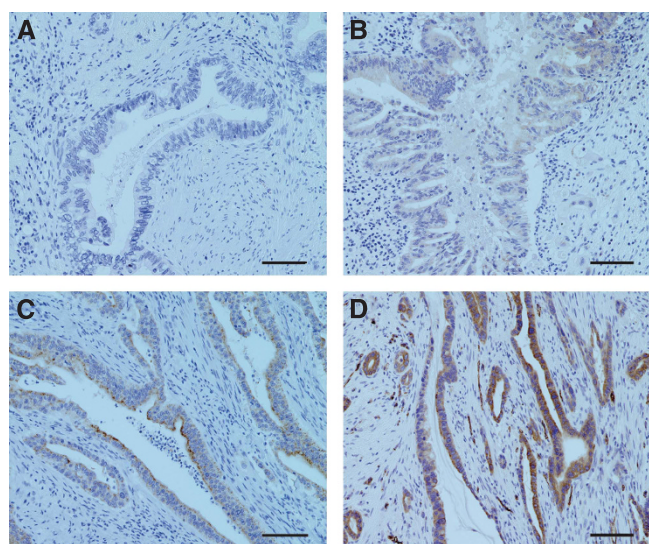

Figure 1. (**A–D**) Representative photomicrographs showing immunohistochemical staining and detailed expression of neuropilin-1 (NRP1, brown colour) in pancreatic ductal adenocarcinomas. Nine (18.8%) cases were negative (IHC-0, **A**), 17 (35.4%) were weakly positive (IHC-1+, **B**), 12 (25.0%) were moderately positive (IHC-2+, **C**), and 10 (20.8%) were strongly positive (IHC-3+, **D**). (**E** and **F**) Kaplan–Meier analysis of overall survival (**E**) and disease-free survival (**F**) in relation to low (IHC-0/1+) or high (IHC-2+/3+) NRP1 expression in pancreatic cancer. Patients with high NRP1 expression showed shorter overall survival (P = 0.0278) and disease-free survival (P = 0.0173) than patients with low NRP1 expression.

Table 1. Correlation between neuropilin-1 (NRP1) expression and clinicopathological parameters of patients with pancreatic cancer

Characteristics	All cases	NRP1 level Low	NRP1 level High	χ^2	P-value
Total participants	48	26	22		
Age at surgery (years)					
<60	14	8	6	0.003	0.958
⩾60	34	18	16		
Gender					
Male	24	13	11	0.084	0.772
Female	24	13	11		
Tumour grade					
Well	2	1	1	0.031	0.985
Moderately	44	24	20		
Poorly	2	1	1		
Tumour location					
Head	40	23	17	0.420	0.517
Body/Tail	8	3	5		
Tumour size					
<40 mm	29	16	13	0.015	0.902
⩾40 mm	19	10	9		
T factor					
T1/T2	2	2	0	1.812	0.404
T3	16	8	8		
T4	30	16	14		
Lymph-node metastasis					
Positive	35	17	18	0.904	0.342
Negative	13	9	4		
Vascular invasion					
Positive	12	4	8	1.790	0.181
Negative	36	22	14		
Perineural invasion					
Positive	24	11	13	0.755	0.385
Negative	24	15	9		
Microvessel density[a]					
<25	16	13	3	5.549	0.018
⩾25	32	13	19		
Resection margin					
Positive	13	7	6	0.089	0.765
Negative	35	19	16		
CEA					
Normal	20	13	7	0.959	0.327
High	28	13	15		
CA19-9					
Normal	16	12	4	3.032	0.082
High	32	14	18		

Abbreviation: CEA = carcinoembryonic antigen.
[a] Number of vessels per 100 magnification field.

hotspots in high-magnification fields (× 200). Four randomly selected regions were analysed and averaged.

Statistical analysis. Values are presented as the means and standard deviation. Statistical analyses were conducted using Dr SPSS II for Windows software (SPSS Inc., Chicago, IL, USA). Differences between groups were assessed statistically using Student's *t*-test or Tukey–Kramer test for parametric data, or the Mann–Whitney *U*-test for non-parametric data. Overall and disease-free survival curves were drawn according to the Kaplan–Meier method, and differences between the curves were analysed by applying the log-rank test. Multivariate Cox regression analysis was used to analyse the independent prognostic factors related to survival. Differences at $P < 0.05$ were considered to be statistically significant.

RESULTS

Correlation of NRP1 overexpression with poor outcome in clinical cases of pancreatic cancer. Neuropilin-1 immunostaining in clinical specimens of pancreatic ductal adenocarcinoma from 48 patients was predominantly identified in the cytoplasm and on the cell surfaces of malignant ductal cells (Figure 1). According to the semi-quantitative assessment criteria employed, the specimens were divided into 4 groups: 9 cases (19.7%) that were negative (IHC-0, Figure 1A), 17 (35.4%) that were weakly immunostained (IHC-1 +, Figure 1B), 12 (25.0%) that were moderately immuno-stained (IHC-2 +, Figure 1C), and 10 (20.8%) that showed strongly positive immunostaining (IHC-3 +, Figure 1D). Compar-isons between low NRP1 expression (IHC-0/1 +) and high NRP1 expression (IHC-2 + /3 +) demonstrated similar clinicopathological features, except for MVD within the tumour ($P = 0.018$, Table 1). The 3- and 5-year survival rates for the 48 patients overall were 54.2% and 12.5%, respectively. Kaplan–Meier analysis demon-strated a significant difference in overall survival between the groups showing high NRP1 expression (median 16.7 months, range 0.5–46.6 months) and low NRP1 expression (median 34.9 months, range 5.6–94.3 months) ($P = 0.0278$, Figure 1E). Disease-free survival also differed significantly between high (median 8.2 months, range 0.5–46.6 months) and low NRP1 expression (median 16.1 months, range 3.2–94.3 months) ($P = 0.017$, Figure 1F). Multivariate analysis using the Cox proportional hazards model indicated that, apart from positivity for lymph-node

metastasis (hazard ratio (HR) = 5.620, 95% confidence interval (CI): 1.312–24.071, $P = 0.020$), involvement of the resection margin (HR = 5.394, 95% CI: 2.227–13.068, $P < 0.001$) and high expression of NRP1 (HR = 2.391, 95% CI: 1.045–5.469, $P = 0.039$) were significantly correlated with poor overall survival, and were independent prognostic factors for pancreatic cancer (Table 2).

iRGD peptide facilitates drug penetration into murine pancreatic cancer models showing NRP1 overexpression. To investigate the activity of iRGD peptide, co-injection of Evans blue dye, and fluorochrome-labelled dextran was performed. Evans blue dye accumulation was enhanced 1.9-fold in two CXs (BxPC-3 and MIA PaCa-2) by co-administration of iRGD; however, enhanced dye accumulation was not observed in the remaining three CXs (Figure 2A; Supplementary Figure S1).

To evaluate the correlation between the iRGD inducing drug penetration effect and NRP1 expression in cancer cells, IHC was performed. Two CXs that showed enhanced dye accumulation were strongly positive (3 +), and the remaining three CXs were weakly positive (1 +) (Figure 2B; Supplementary Figure S2).

Three CXs (BxPC-3, MIA PaCa-2, and SUIT-2) and three TGs that showed NRP1 overexpression (Supplementary Figure S2) were employed in dextran experiments. Co-administration of iRGD peptide induced the dextran penetration into tumour parenchyma compared with dextran single administration (Figures 2C and D). Extended dextran-positive areas in CXs were 1.8-fold in BxPC-3 ($P = 0.001$) and 2.1-fold in MIA PaCa-2 ($P = 0.024$), but had no effect in SUIT-2 (Figure 2E). Penetration of dextran by co-administration of iRGD peptide was also observed in TGs, the areas of dextran distribution were extended 1.7-fold in PC-03 ($P = 0.008$), 3.0-fold in PC-09 ($P = 0.001$), and 1.9-fold in PC-10 ($P = 0.040$) (Figure 2E).

Enhancement of the anticancer effect by co-administration of GEM and iRGD peptide in comparison with GEM monotherapy. Enhanced drug penetration into tumour was evaluated by Evans blue dye as a drug substitute tracer (Figure 3A). Drug accumula-tions in two CXs and one TG (PC-03) were significantly enhanced by iRGD co-administration; however, the effects in other two TGs (PC-09 and 10) were not remarkable. Similarly, co-administration of iRGD with GEM significantly decreased tumour growth in comparison with GEM monotherapy in BxPC-3 ($P = 0.046$, Figures 3B and C) and MIA PaCa-2 ($P = 0.037$, Figure 3C). One TG model (PC-03) also showed a significant tumour growth

Table 2. Cox proportial hazards model of prognostic factors in patients with pancreatic cancer ($n = 48$)						
	Univariate analysis			**Multivariate analysis**		
Factor	**HR**	**95% CI**	**P-value**	**HR**	**95% CI**	**P-value**
Age (≥60 years)	0.934	0.418–2.084	0.867	NA	NA	NA
Gender (male)	0.885	0.415–1.887	0.752	NA	NA	NA
T factor (T4)	1.433	0.642–3.199	0.380	NA	NA	NA
Tumour size (≥40 mm)	2.166	1.010–4.646	0.047	1.738	0.748–4.042	0.199
Lymph-node status (positive)	6.712	1.585–28.421	0.010	5.620	1.312–24.071	0.020
Vascular invasion (positive)	1.768	0.769–4.068	0.180	NA	NA	NA
Perineural invasion (positive)	1.726	0.797–3.740	0.166	NA	NA	NA
Resection margin (positive)	5.757	2.501–13.251	<0.001	5.394	2.227–13.068	<0.001
Microvessel density[a] (≥25)	1.214	0.543–2.715	0.637	NA	NA	NA
Neuropilin-1 expression (high)	2.334	1.072–5.083	0.033	2.391	1.045–5.469	0.039

Abbreviations: CI = confidence interval; HR = hazard ratio; NA = not applicable.
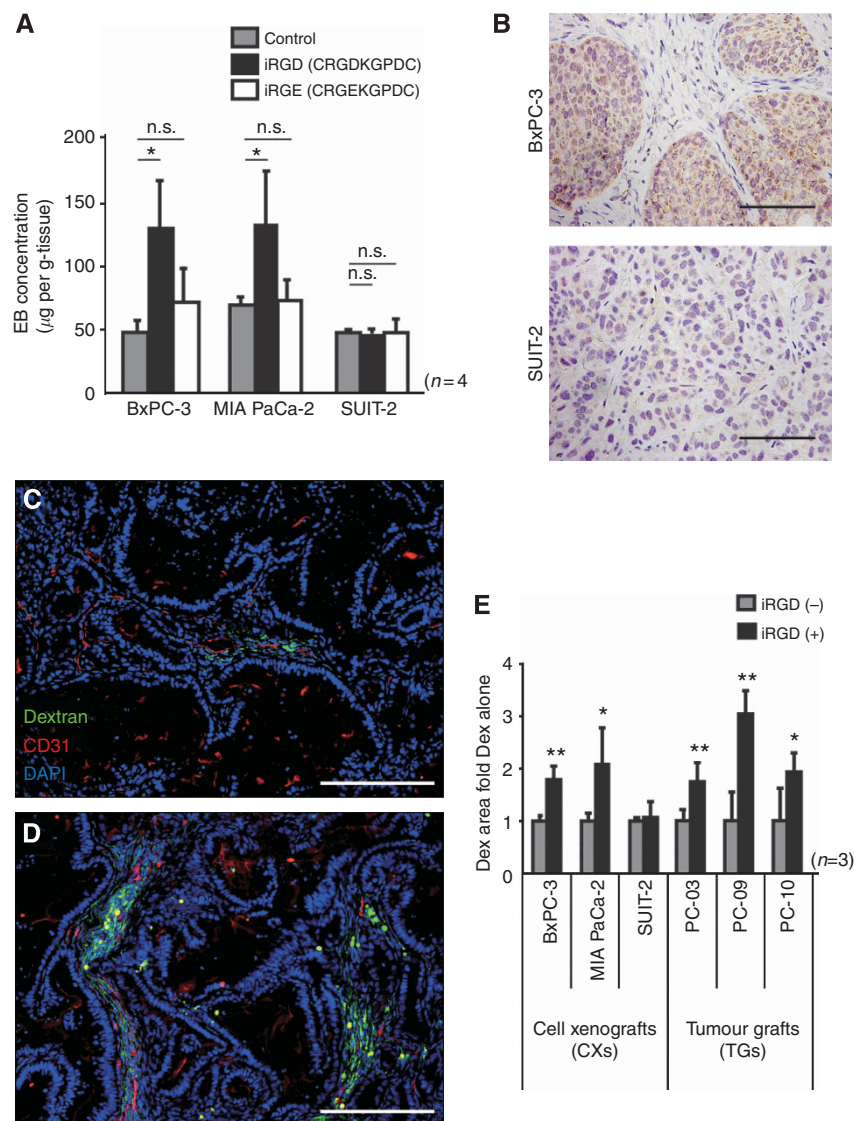[a]Number of vessels per 100 magnification field.

Figure 2. (A) Evans blue dye accumulation assay for cell line-based xenograft models (cell xenografts: CXs). Co-administration of iRGD peptide with a drug (black bar) was compared with administration of a single drug alone (grey bar) or iRGE peptide (white bar). Dye accumulation was enhanced 1.9-fold in BxPC-3 and MIA PaCa-2, but not in SUIT-2. Control peptide (iRGE) showed no enhancement of dye accumulation (N = 4 per group). (B) Neuropilin-1 (NRP1) expression in animal models (×400 magnification; scale bar, 100 μm). Overexpression of NRP1 was shown in BxPC-3 (upper) and MIA PaCa-2 (not shown), but not in SUIT-2 (lower). (C and D) Distribution of fluorochrome (Alexa-488, green)-labelled dextran in frozen sections of PC-09 (×200 magnification; scale bar, 200 μm). Tumour vasculature was stained with anti-CD31 antibody (red), and nuclei were stained with DAPI (blue). Dextran appeared faintly after single administration (C), and it was more widely distributed with a stronger intensity after co-administration with iRGD peptide (D). (E) The areas of dextran distribution were calculated and compared. iRGD co-administration increased the area of dextran distribution 1.8-fold in BxPC-3 (P = 0.001), 2.1-fold in MIA PaCa-2 (P = 0.024), 1.7-fold in PC-03 (P = 0.008), 3.0-fold in PC-09 (P = 0.001), and 1.9-fold in PC-10 (P = 0.040). *P < 0.05, **P < 0.01.

suppression by the combination therapy (P = 0.048), but the other two TGs (PC-09 and 10) exhibited no significant differences (Figure 3C). The body weight of mice was decreased on days 12 and 15 in the GEM administered groups relative to the control group, but there was no significant difference in body weight between the iRGD co-administration group and the GEM monotherapy group (data not shown).

DISCUSSION

The present study conducted to re-evaluate the use of iRGD peptide demonstrated that it boosted the accumulation of drugs in two of five pancreatic cancer CXs that showed high expression of

NRP1, and the anticancer effects of GEM were also enhanced by iRGD co-administration in these two CXs. We concluded that iRGD co-administration therapy would be indicated for nearly half of all patients with pancreatic cancer showing NRP1 over-expression, and we further evaluated this possibility using clinically relevant murine pancreatic cancer TG models. Enhancement of drug accumulation by iRGD was also observed in TGs, but the effects were less marked than those in CXs. Additionally, a significant anticancer booster effect of GEM plus iRGD combination therapy was observed in only one model.

First, our experiments using five CXs reconfirmed the enhanced drug accumulation effect of iRGD peptide. It was noteworthy that our experiments demonstrated that the effect of iRGD was dependent on the level of NRP1 expression; that is, the effects of iRGD were marked in two high-NRP1 CXs, but not significant in
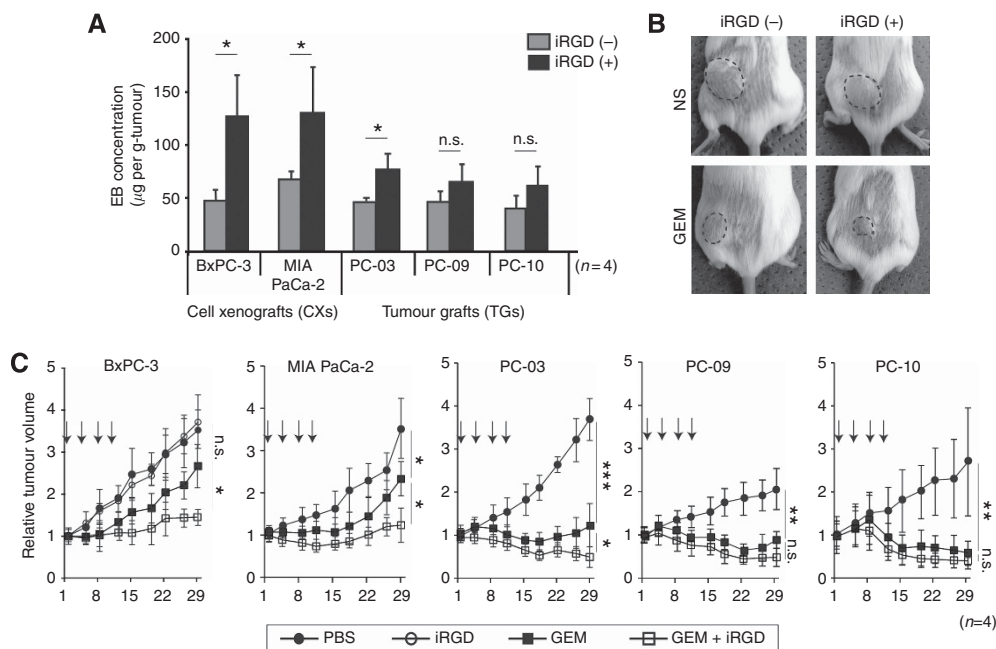
Figure 3. Tumour treatment studies involving co-administration of iRGD peptide. (A) Enhanced drug accumulation into tumour using Evans blue dye as a drug substitute tracer. Drug accumulations were enhanced about twofolds by iRGD in two CXs and one TG; however, the effects were not significant in another two TGs. (B) Tumour appearances in ectopic BxPC3 models at 28 days after the treatment initiation. (C) Tumour growth curves of gemcitabine (GEM) and iRGD combination therapy. Tumour-bearing mice were injected with 100 mg kg^{-1} gemcitabine or 100 μl of PBS (twice per week for 2 weeks; days 1, 4, 8, and 11; arrows show the day of infusion) combined with injection of PBS (Control, and GEM groups) or 8 μmol kg^{-1} iRGD peptide (iRGD, and GEM + iRGD group) 10 min beforehand ($N = 4$ per group). Tumour growth curves of two CXs (BxPC-3 and MIA PaCa-2) and three TGs (PC-03, PC-09, and PC-10) are indicated. *$P < 0.05$, **$P < 0.01$, ***$P < 0.001$; n.s., not statistically significant.

three low-NRP1 models. These results suggest that iRGD peptide co-administration would be beneficial for subset patients with NRP1-overexpressing tumours, similarly to a molecular targeting agent.

We then evaluated the populations of pancreatic cancer overexpressing NRP1 in clinical specimens. Neuropilin-1 over-expression was seen in 45.8% of specimens, and the patients concerned had worse outcomes than patients whose tumours had low NRP1 expression (Figures 1E and F). Neuropilin-1 is known to be a co-receptor that enhances the binding of VEGF-A to the VEGF receptor (Soker et al, 1998), and NRP1 overexpression induces upregulation of VEGF signalling that is associated with angiogenesis and cancer metastases (Poon et al, 2001). Our finding that NRP1 overexpression was associated with higher MVD (Table 1) was considered to reflect upregulation of VEGF signalling. However, it should also be noted that resistance to GEM might have contributed to the differences in outcome. Neuropilin-1-overexpressing pancreatic cancer cell lines showed chemoresistance to GEM in vitro (Wey et al, 2005). All of the patients included in our study had received GEM-based adjuvant chemotherapy, and the effects of drug resistance should therefore be considered.

The effect of iRGD peptide in enhancing drug penetration is expected to improve the efficacy of treatment for dismal solid tumours, including pancreatic cancer. However, CXs do not adequately represent the clinical features of pancreatic cancer. We therefore employed pancreatic TGs, which have been reported to show better clinical predictive ability (Dong et al, 2010; Hidalgo et al, 2011; Morelli et al, 2012), and our previous evaluation had indicated that the drug delivery characteristics of TGs were more clinically reproducible. Histological findings of pancreatic TGs were more similar to clinical pancreatic cancer compared with CXs, as showing the atypical cancer glands and stromal tissues (Supplementary Figure S2). Internalised-RGD peptide certainly

induced drug penetration in all TGs that were overexpressed NRP1, combination therapy using iRGD peptide was considered to be applicable for clinical pancreatic cancer.

Finally, the efficacy of iRGD peptide co-administration with GEM was verified using five pancreatic cancer models that showed enhanced drug accumulation in dextran experiments. In three models, iRGD peptide significantly enhanced drug accumulation into tumour (Figure 3A). Anticancer effect of GEM was also enhanced by iRGD co-administration in these three models (Figure 3C). Therefore, it seems possible to co-administer GEM, which is a key first-line drug for pancreatic cancer, with iRGD peptide, though the molecular size of GEM (0.3 kDa) is smaller than that of agents previously validated (0.6 kDa–130 nm, Sugahara et al, 2010). On the other hand, enhanced drug accumulations by iRGD peptide in the remaining two TGs were limited (Figure 3A), and the anticancer effects were also not significantly enhanced (Figure 3C). A major factor influencing the results was considered to be different histological findings among these models. Drug penetrations around the perfusing tumour vessels were not so different between CXs and TGs as shown in dextran experiments (Figure 2E). However, TGs included relative fewer blood vessels and more stromal tissues like clinical pancreatic cancer, as we previously reported (Akashi et al, 2013). We therefore considered that the efficacy of iRGD co-administration might be limited in clinical pancreatic cancer, characterised as poor vascularity and prominent desmoplastic reaction. A TG model (PC-03) that showed significant effect of iRGD peptide was established by transplantation of liver metastatic cancer tissue, whereas the other two TGs (PC-09 and 10) were established from primary pancreatic cancer. Histological findings of PC-03 (Supplementary Figure S2) were relatively similar to CXs, as characterised as hypervascular and fewer stromal tissues (Supplementary Figure S2; Akashi et al, 2013). Paradoxically, it is presumed that the impact of histological features on the iRGD efficacy is greater. Though the difference of

drug susceptibility between CXs and TGs should be accounted for the interpretation of our results. As shown in Figure 3C, GEM monotherapy showed <50% inhibition of tumour growth in two CXs. In contrast, tumour growths in both TGs were significantly supressed by GEM monotherapy. Therefore, further validations, such as experiments using GEM-resistant TGs, might be required.

Our re-evaluations of iRGD peptide demonstrated a substantial booster accumulation effect of drugs in mouse pancreatic cancer models with high NRP1 expression, and this effect may be exploitable in nearly half of all patients with pancreatic cancer showing high NRP1 expression. Since the booster anticancer effects of iRGD co-administration with GEM were marked only in cell line-based models but not so great in TGs, the possible clinical application of iRGD peptide should be considered carefully.

ACKNOWLEDGEMENTS

CONFLICT OF INTEREST

The authors declare no conflict of interest.

REFERENCES

Akashi Y, Oda T, Ohara Y, Miyamoto R, Hashimoto S, Enomoto T, Yamada K, Kobayashi A, Fukunaga K, Ohkochi N (2013) Histological advantages of the tumor graft, a murine model involving transplantation of human pancreatic cancer tissue fragments. *Pancreas* **42**: 1275–1282.

Burris 3rd HA, Moore MJ, Andersen J, Green MR, Rothenberg ML, Modiano MR, Cripps MC, Portenoy RK, Storniolo AM, Tarassoff P, Nelson R, Dorr FA, Stephens CD, Von Hoff DD (1997) Improvements in survival and clinical benefit with gemcitabine as first-line therapy for patients with advanced pancreas cancer: a randomized trial. *J Clin Oncol* **15**: 2403–2413.

Dong X, Guan J, English JC, Flint J, Yee J, Evans K, Murray N, Macaulay C, Ng RT, Gout PW, Lam WL, Laskin J, Ling V, Lam S, Wang Y (2010) Patient-derived first generation xenografts of non-small cell lung cancers: promising tools for predicting drug responses for personalized chemotherapy. *Clin Cancer Res* **16**: 1442–1451.

Fukahi K, Fukasawa M, Neufeld G, Itakura J, Korc M (2004) Aberrant expression of neuropilin-1 and -2 in human pancreatic cancer cells. *Clin Cancer Res* **10**: 581–590.

Hansel DE, Wilentz RE, Yeo CJ, Schulick RD, Montgomery E, Maitra A (2004) Expression of neuropilin-1 in high-grade dysplasia, invasive cancer, and metastases of the human gastrointestinal tract. *Am J Surg Pathol* **28**: 347–356.

Heldin CH, Rubin K, Pietras K, Ostman A (2004) High interstitial fluid pressure - an obstacle in cancer therapy. *Nat Rev Cancer* **4**: 806–813.

Hidalgo M, Brunckheimer E, Rajeshkumar NV, Garrido-Laguna I, De Oliveira E, Rubio-Viqueira B, Strawn S, Wick MJ, Martell J, Sidransky D (2011) A pilot clinical study of treatment guided by personalized tumorgrafts in patients with advanced cancer. *Mol Cancer Ther* **10**: 1311–1316.

Jain RK (1999) Transport of molecules, particles, and cell in solid tumors. *Annu Rev Biomed Eng* **1**: 241–263.

Kolodkin AL, Levengood DV, Rowe EG, Tai YT, Giger RJ, Ginty DD (1997) Neuropilin is a semaphorin III receptor. *Cell* **90**: 753–762.

Li M, Yang H, Chai H, Fisher WE, Wang X, Brunicardi FC, Yao Q, Chen C (2004) Pancreatic carcinoma cells express neuropilins and vascular endothelial growth factor, but not vascular endothelial growth factor receptors. *Cancer* **101**: 2341–2350.

Morelli MP, Calvo E, Ordoñez E, Wick MJ, Viqueira BR, Lopez-Casas PP, Bruckheimer E, Calles-Blanco A, Sidransky D, Hidalgo M (2012) Prioritizing phase I treatment options through preclinical testing on personalized tumorgraft. *J Clin Oncol* **30**: e45–e48.

Müller MW, Giese NA, Swiercz JM, Ceyhan GO, Esposito I, Hinz U, Büchler P, Giese T, Büchler MW, Offermanns S, Friess H (2007) Association of axon guidance factor semaphorin 3A with poor outcome in pancreatic cancer. *Int J Cancer* **121**: 2421–2433.

Parikh AA, Liu WB, Fan F, Stoeltzing O, Reinmuth N, Bruns CJ, Bucana CD, Evans DB, Ellis LM (2003) Expression and regulation of the novel vascular endothelial growth factor receptor neuropilin-1 by epidermal growth factor in human pancreatic carcinoma. *Cancer* **98**: 720–729.

Poon RT, Fan ST, Wong J (2001) Clinical implications of circulating angiogenic growth factors in cancer patients. *J Clin Oncol* **19**: 1207–1225.

Ruoslahti E, Bhatia SN, Sailor MJ (2010) Targeting of drugs and nanoparticles to tumors. *J Cell Biol* **188**: 759–768.

Sobin LH, Gospodarowicz MK, Wittekind C (2009) *TNM Classification of Malignant Tumours.* 7th edn. Wiley-Blackwell: Chichester, UK.

Soker S, Fidder H, Neufeld G, Klagsbrun M (1996) Characterization of novel vascular endothelial growth factor (VEGF) receptors on tumor cells that bind VEGF165 via its exon 7-encoded domain. *J Biol Chem* **27**: 5761–5767.

Soker S, Takashima S, Miao HQ, Neufeld G, Klagsbrun M (1998) Neuropilin-1 is expressed by endothelial and tumor cells as an isoform-specific receptor for vascular endothelial growth factor. *Cell* **92**: 735–745.

Sugahara KN, Teesalu T, Karmali PP, Kotamraju VR, Agemy L, Girard OM, Hanahan D, Mattrey RF, Ruoslahti E (2009) Tissue-penetrating delivery of compounds and nanoparticles into tumors. *Cancer Cell* **16**: 510–520.

Sugahara KN, Teesalu T, Karmali PP, Kotamraju VR, Agemy L, Greenwald DR, Ruoslahti E (2010) Coadministration of a tumor-penetrating peptide enhances the efficacy of cancer drugs. *Science* **328**: 1031–1035.

Teesalu T, Sugahara KN, Kotamraju VR, Ruoslahti E (2009) C-end rule peptides mediate neuropilin-1-dependent cell, vascular, and tissue penetration. *Proc Natl Acad Sci USA* **106**: 16157–16162.

Tempero M, Plunkett W, Ruiz Van Haperen V, Hainsworth J, Hochster H, Lenzi R, Abbruzzese J (2003) Randomized phase II comparison of dose-intense gemcitabine: thirty-minute infusion and fixed dose rate infusion in patients with pancreatic adenocarcinoma. *J Clin Oncol* **21**: 3402–3408.

Wey JS, Gray MJ, Fan F, Belcheva A, McCarty MF, Stoeltzing O, Somcio R, Liu W, Evans DB, Klagsbrun M, Gallick GE, Ellis LM (2005) Overexpression of neuropilin-1 promotes constitutive MAPK signalling and chemoresistance in pancreatic cancer cells. *Br J Cancer* **93**: 233–241.

Supplementary Information accompanies this paper on British Journal of Cancer website (http://www.nature.com/bjc)